S- and N-doped carbon quantum dots: Surface chemistry dependentantibacterial activity

Nikolina A. Travlou [a, b], Dimitrios A. Giannakoudakis [a, b], Manuel Algarra [c, d], Alejandro M. Labella [e], Enrique Rodríguez-Castellón [c], Teresa J. Bandosz [a, b, *]

[a] *Department of Chemistry, The City College of New York, New York, NY, 10031, USA*
[b] *Ph.D. Program in Chemistry, The Graduate Center of the City University of New York, New York, NY, 10016, USA*
[c] *Department of Inorganic Chemistry, Faculty of Science, The University of Malaga, Campus de Teatinos, 29071, Málaga, Spain*
[d] *Madeira Chemistry Research Centre-CQM, University of Madeira, Campus de Penteada, 9020-105 Funchal, Portugal*
[e] *Department of Microbiology, Faculty of Science, The University of Malaga, 29071, Málaga, Spain*

* Corresponding author. Department of Chemistry and Biochemistry, The CityCollege of New York, New York, NY, 10031, USA.
E-mail address: tbandosz@ccny.cuny.edu (T.J. Bandosz).

ABSTRACT

Sulfur and nitrogen-doped carbons quantum dots (S-CQDs and N-CQDs) were obtained using a simple hydrothermal treatment of S- or N-containing organic compounds/polymers. They were evaluated for their bactericidal activity against representative Gram-negative (*Escherichia coli,* CECT 831) and Gram-positive (*Bacillus subtilis* subsp. *subtilis* 168) bacterial strains, using a qualitative estimation approach. Quantitative tests revealed greater effectiveness of N-CQDs compared to S-CQDs. The bactericidal activity of the dots was linked to their specific surface chemistry, and their sizes in the range of nanometers. Inthe case of the N-CQDs, amides and amines played the most important role in enhancing bactericidal function. They caused a bacterial death which was linked to the electrostatic interactions between their protonated forms and the lipids of the bacterial cell membrane. It is also possible that the ability to activate oxygen species by the CQDs surface played some role. S-CQDs showed a much lower bactericidal activity compared to that of N-CQDs. These dots (S-CQDS), containing mainly a negatively charged surface due to dissociation of sulfonic/carboxylic groups and sulfates, showed a size dependent rather than a chemistry dependent (electrostatic interactions) inhibition of the Gram-positive bacterial growth. This is the first study where the role of different heteroatoms incorporated to CQDs is examined in the context of the bactericidal activity.

1. Introduction

The preparation of materials with high antibacterial activity/ properties (for public life protection) is a major challenge. Metal ions, quaternary ammonium compounds, and antibiotics are well known to reduce or inhibit the microbial/bacterial cell viability [1-3]. Nevertheless, high costs, complex chemical synthetic routes, resistance to antibiotics, or the environmental pollution are some potential problems/limitations associated with the usage of the above-mentioned and established bactericides or bacteriostatic substances [4]. Carbon quantum dots (CQDs) as alternatives to semiconductor quantum dots, are a new class of metal-free fluorescent nanoparticles that have attracted the interest of scientists because of their simple synthesis, low toxicity, good biocompatibility, and easiness of surface modifications [5,6]. They consist of a fraction of nanometer-sized carbon core surrounded by amorphous carbon frames. Their surface functional groups (eg. hydroxyl, carboxyl, epoxy, amino, amides, etc.) can serve as reactive sites. Because of their unique properties and especially low toxicity and biocompatibility, they have found numerous applications in various fields including bacterial imaging/sensing, drug/gene delivery, catalysis, and sensing [7-10]. So far, various methods have been reported forthe synthesis of CQDs, which can be generally classified in two categories: a) the top-down route, which refers to the preparation of CQDs breaking down larger carbon materials through chemical oxidation, laser-ablation, or electrochemical synthesis [5,11] and b) the bottom-up route, which includes the preparation of CQDs from smaller precursors applying hydrothermal/solvothermal treatments, microwave/ultrasonic preparation routes, or plasma treatment [11-13].

Quantum dots (QDs) have been tested as bactericides and it hasbeen reported in several studies that the main operation principle behind their microbial activity are the interactions between the dotnanoparticles and the bacteria [7,14]. Considering that the toxicity of QDs depends on their size and surface charge, these properties can be easily tuned/controlled through surface functionalization [14]. In the case of CQDs, on the other hand, even though numerousinvestigations have been reported on their various biological applications [5,15-17], their bactericidal activity is still debatable andnot explained in details.

Very few studies have been reported on the antibacterial function of graphene quantum dots (GQDs), which, due to their basal plane structure similar to that of graphite/graphene oxide, are also referred to as GO-GQDs [18]. Some studies have demonstrated the inactivity of GQDs against a wide range of bacteria [18,19]. Hui andcoworkers however found that GQDs synthesized by rupturing C_{60} cage (C_{60}-GQD) show bactericidal activity towards a specific bacterial strain (*Staphylococcus aureus*) [18]. They lack, however, the same activity towards other bacterial strains such as *Escherichia coli*, *Bacillus subtilis*, or *Pseudomonas aeruginosa*. Another study byRistic and coworkers [19] demonstrated that electrochemically produced GQDs exhibit photodynamic antibacterial activity to- wards two different bacterial strains (*S. aureus* and *E. coli*). Even fewer studies report the antibacterial activity of pure carbon quantum dots. Roy and coworkers reported that CQDs derivedby resorcinol and formaldehyde resins show sufficient bactericidal activity. However, it happens only when they are decorated with Agnanoparticles [20]. The latter (Ag-NPs)

are known for their strong antibacterial activities [21,22]. Some other studies have shown that quaternized (with quaternary ammonium groups) carbon dots exhibit antimicrobial activity, especially towards Gram-positive bacteria. This is related to the electrostatic interactions of cationic molecules with the surface of the bacterial cells. Yang and co- workers fabricated quaternized CQDs through a simple carboxyl- amine reaction between amine-functionalized CQDs and a qua-ternary ammonium compound (lauryl betaine) [7]. They found that the obtained CQDs showed a good antibacterial activity, which was linked to the selective attachment of the positively charged qua- ternary ammonium groups to the negatively charged surface of a Gram-positive bacterial strain. Similar observations have been re- ported by Dou and coworkers [23] who also showed that quarte- nization of CQDs, derived from glucose and poly (ethyleneimine) (PEI), led to the bactericidal function of the dots. This is in agree- ment with even earlier studies, which demonstrated that quater- nized polymers and quaternary ammonium compounds (QACs) exhibit strong bactericidal activity against Gram positive bacteria [24,25].

The surface charge of carbon dots has been reported as an important factor controlling their bactericidal activity. The mech- anism behind the bactericidal effect of charged dots has been linked to their ability to disrupt the cell-membrane integrity [26]. Bing and co-workers examined the death of bacteria caused by CQDs with different surface charges [14]. They found that while positively and negatively charged dots acted as bactericides towards *E. coli*, un- charged dots were inactive. Upon the interaction of the charged dots with the bacteria, the main factor responsible for the inhibi- tion of the bacterial growth was the generation of reactive oxygen species (ROS), such as hydroxyl radicals [27]. In another study by Meziani and coworkers [28], the photoinduced bactericidal func- tion of carbon quantum dots was reported. The capability of the dots to cause bacterial death was linked to their activation by visible light. The authors, however did not examine the link be- tween the light-activated bactericidal function of the dots and their structural and surface chemical features, and they set it as a subject for further investigation.

Since recently extensive studies have been carried out on the bactericidal properties of other graphene-based nanomaterials, such as graphene, graphene oxide (GO), reduced graphene oxide (rGO), and carbon nanotubes (CNTs) [18,29-31], there is also a need for a systematic investigation of the surface chemistry-antibacterial properties of carbon dots as bactericides. Unlike various metals or metal oxides used as bactericidal agents, the carbon-based mate- rials are easier to obtain and are more economic [30]. Nevertheless, in their case, certain limitations related to their interactions with cells exist. In the case of graphene and its derivatives, graphene induced cell degradation has been reported to be linked to both physical and chemical processes. The latter ones include the oxidative stress through the generation of reactive oxygen species (ROS), while the former one involves the cell damage caused by the sharp edges of the graphene nanosheets [32]. The main drawback of such graphene-based materials is that graphene can cause cell apoptosis or necrosis by affecting the DNA of the cells and the mitochondrial activity [33]. Moreover, in the case of CNTs, even though they can easily penetrate the cell membranes and act as bactericidal agents, they exhibit some cytotoxicity towards both bacterial and human cells. Thus, the investigation of biocompatible carbon nanomaterials as bactericidal agents seems to be a necessity in the biological/environmental field.

Considering that the surface chemistry of CQDs should not significantly differ from that of other forms of carbon, their anti- bacterial activity might be influenced by the same chemical fea- tures as those of carbon particles, and more precisely by the specific configuration of certain heteroatoms. In that case, the effect of a specific heteroatom configuration on the bactericidal activity of CQDs could be explained based on the effect of the same hetero- atoms on the catalytic activity [34-36]. In many cases, especially for nitrogen doped carbons [35], that catalytic activity has been linked to the formation/generation of superoxide ions (O_2^-).

The objective of this paper is to examine if heteroatom-decorated CQDs exhibit antibacterial activity, and if so, how it is linked to their specific surface chemistry (specific configuration of the heteroatoms). For this purpose, a simple hydrothermal treat- ment of sulfur or nitrogen containing organic compounds/polymers was applied to obtain S-CQDs and N-CQDs, respectively. To study the antibacterial properties of S- and N-CQDs, *Bacillus subtilis* as a representative Gram-positive, and *Escherichia coli* as a representa-tive Gram-negative strain were used as the targets. The results obtained present both, qualitative (disk diffusion tests) and quan- titative (minimal inhibitory concentration, MIC) effects of CQDs onto bacterial growth. The role of the specific surface chemistry (specific configuration of the heteroatoms) was then extensively analyzed and linked to the antibacterial capability of the dots. The S-containing CQDs were described in our previous study (referred to as S1-CQDs) [37] where we tested their ammonia detection capability based on the fluorescence quenching.

2. Experimental

2.1. Preparation of materials

For the preparation of the S-CQDs and N-CQDs, poly (sodium- 4- styrene sulfonate) or polyvinylpyrrolidone were used as the sulfur or nitrogen sources, respectively. Predetermined amounts of the two polymers were first dissolved in 50 mL of H_2O, and the solu- tions were then added to Teflon-

lined stainless steel autoclaves. The autoclaves were heated to 200 °C for 6 h. For the purification of the obtained dots, the obtained mixtures were first filtered using a cylindrical filtration membrane filter (0.22 mm), which was followed by their extensive washing with dichloromethane, for the removal of organic moieties. The dichlormethane phase (heavier than water) was removed using a separation funnel. Finally, the less fluorescent deposit was separated by centrifuging the solutions at 8000 rpm for 15 min. To obtain dry samples for further analyses (surface chemistry) water was evaporated by slowly heating the solutions at 80 °C.

2.2. Methods

2.2.1. FT-IR spectroscopy

Fourier transform infrared (FTIR) spectra were collected using a Nicolet Magna-IR 830 spectrometer, with the attenuated total reflectance method (ATR) on the powdered samples (without KBr addition). The spectra were collected 64 times and corrected for the background noise.

2.2.2. High-resolution transmission electron microscopy (HRTEM):

The morphology of S,N-CQDs was analyzed by high trans- mission electron microscopy (HRTEM) and examined under a FEI Talos F200X.

2.2.3. XPS

XPS studies were performed on a Physical Electronic PHI 5700 spectrometer using non-monochromatic Mg-K_a radiation (300 W, 15 kV and 1253.6 eV) for analysing the core-level signals of the el- ements of interest with a hemispherical multichannel detector. The sample spectra were recorded with a constant pass energy value at 29.35 eV, using a 720 mm diameter circular analysis area. The X-ray photoelectron spectra obtained were analyzed using PHI ACESS ESCA-V6.0F software and processed using MultiPak 8.2B package. The binding energy values were referenced to adventitious carbon C 1*s* signal (284.8 eV). Shirley-type background and Gauss-Lorentz curves were used to determine the binding energies.

2.2.4. Fluorescence spectroscopy

Fluorescence measurements of the aqueous solutions were made using a 1 cm square quartz cuvette in a spectrophotomer (Fluoromax, Horiba Inc). For intensity comparison, the emission intensity was corrected for excitation power. The excitation- emission scans were made with an excitation increment of 5 nm.

2.2.5. Strains and growth conditions

Wild type strains of Escherichia coli (MG1655) and Bacillus sub- tilis (ATCC 6051) were used in the antimicrobial disk diffusion as- says. Bacteria were grown at 37 ◦C in Mueller-Hinton agar and/or both media (HiMedia Laboratories).

2.2.6. Antimicrobial disk diffusion assays

Optical densities (OD_{600}) of overnight cultures of bacteria were determined and diluted to obtain 10^8 CFU/mL bacterial counts. A 100 mL aliquot of the diluted bacterial culture was evenly spread on a Muller Hinton agar plate. Next, sterile filters (7 mm diameter, Whatman) soaked in either the buffer alone, or the carbon quan- tum dot (CQD) suspensions of 2.9% w/v in concentration, were placed onto these bacterial spread plates and then incubated at 37 °C for ~16 h, in the dark. The diameters of the zone of inhibition of bacterial growth were measured.

2.2.7. Minimal inhibitory concentration (MIC) test

Overnight grown cultures of Escherichia coli CECT 831 or Bacillus subtilis subsp. subtilis 168 cells were used to prepare the initial bacterial cell suspensions using trypticase soy broth (TSB, Oxoid) with an incubation temperature of 37 ◦C 3 h. Bacterial cells were washed twice with saline solution and adjusted to a concentration of 6 × 106 cells/ml. The bacterial growth measurement was per- formed in 96-well plates. Each well contained 50 mL of bacteria cell suspension and various concentrations (0.5,1, 2, 4, 8, 16 and 32 mg/ mL) of S-CQDs and N-CQDs (prepared after drying the CGES and their dissolution) in 100 mL of TSB for a final volume of 150mL/well. The analysis was performed in triplicate. The treated bacterial samples were then incubated at 37 ◦C for 24 h. The optical densities (OD) of the samples were measured at wavelength 595 nm after incubation using Eon™ High Performance Microplate Spectro- photometer (BioTek) with the software GenS v.2.05. Inhibitory ef- fect of treatment on bacterial growth can be evaluated based on a decrease in the OD595 values compared to those for the untreated control samples.

2.2.8. z potential measurements

The zeta potential (z) of N,S-CQDs was determined using a Zetasizer Nano ZS (Malvern Instruments, U.K.) equipped with a 4 mW HeNe laser operating at l ¼ 633 nm. The z measurements were also performed at 25 ◦C in polycarbonate folded capillary cells, incorporated with Au plated electrodes (DTS1061) and deionized H2O was the dispersion medium. z were automatically obtained by the software, using the Stokes-Einstein and the Henry equation, with the Smoluchowski approximation.

3. Results and discussion

3.1. Antibacterial activity of N-CQDs and S-CQDs

The antibacterial activities of S-CQD and N-CQDs were tested qualitatively against representative Gram-negative (*E. coli*) and Gram-positive (*B. subtilis*) bacteria in disk diffusion assays. In such tests, the diameter of the inhibition zone is indicative of the susceptibility of the microorganism to a specific material that has antimicrobial properties to a tested group of bacteria. Thus, the more susceptible the strain is to the antimicrobial action of the compound, a larger diameter of the inhibition zone is expected. The disk diffusion data are presented in Fig. 1. For N-CQDs, the anti- bacterial activity is slightly higher against the Gram-positive *B. subtilis* than against Gram-negative *E. coli*. Similar enhancement of antibacterial activity against the Gram-positive *B. subtilis* was also found for S-CQDs, however, their activity against the Gram-negative *E. coli*), was found minimal.

The range of the inhibition zones of the dots and water itself (solvent) measured against Gram-negative and Gram-positive model bacteria are compared and illustrated in the bar graph in Fig. S1 and Table S1 of the Supplementary Information (S.I.).

Since the disk test rather presents the antibacterial activity qualitatively than quantitatively, the inhibitory effects were quantitatively estimated in determination on MIC of CQDs effect on the bacterial growth. The results are presented in Fig. 2. As seen, the different concentrations of S-CQDs and N-CQDs (0.5e32 mg/mL) differ in their inhibitory effects on the growth of *E. coli* and *B. subtilis.* The measured OD values were compared to those for the positive (stationary growth phase reached by each bacterial group) and negative (each CQDs concentration in broth culture medium (TSB) and DMEM where CQDs were initially resuspended) controls. MICs were estimated for N-CQDs and S-CQDs as the minimal concentration where OD values were similar to those obtained for the negative control. Even though the effect of both CQDs on the growth of *E. coli* seems to be stronger than that on *B. subtilis*, the MIC values for both CQDs were 32 mg/mL. The latter bacteria ap- pears as more affected even at lower concentration of CQDs. Thus a 25% decrease in *B. subtilis* growth was found even at 0.5 mg/mL of N-CQDs that shows the stronger effect than that of S-CQDs. At the concentration of 8 mg/mL the effects are similar and the growth inhibition reaches 50% at 16 mg/mL. The results at 32 mg/mL for *B. subtilis* are not interpreted. The large discrepancy in the results measured is associated to a high concentration of CQDs. In the presence of gram positive *B. subtilis* some aggregation effects is found, which affected the optical density measurements. That ef- fect of low concentration of CQDs and the difference in their effects on *B. subtilis* are consistent with the disk inhibition results. On the other hand, small or lack of the effect of CQDs on disk test on *E. coli* is likely caused by too low concentration of CQDs used in that qualitative analysis. In addition, while the effect of both CQDs on *E. coli* are similar, S- and N-CQDs appears as more active to inhibit the growth of *B. subtilis* than that of *E. coli* at 16 mg/mL [38]. It is important to mention that when ceftiofur, enrofloxacin, gentamicin, and trimethoprim/sulfadiazine were tested against *E. coli* strains, the most active compounds with MIC at which 50% of the strains were at or below (MIC50) were 0.5, < or ¼ 0.03, 0.5, and 0.13 mg/mL, respectively. MIC90 were 1.0, 0.13, 32.0, and 2.0 mg/mL, respectively. For other antibiotics as ampicillin, florfenicol, neomycin, and spectinomycin MIC90 > 32.0, 8.0, 512.0, and >128.0 mg/mL. Apparently, in this comparison, our CQDs are equal or better inhibitors for *E. coli* than the most common antibiotics. Moreover, silver nanocomposite was reported as exhibiting MIC of 62.5 mg/mL against *E. coli* [39]. MICs of various *Bacillus subtilis* were found sensitive to tetracycline (MIC90e8.0 mg/mL), vancomycin (MIC90e4.0 mg/mL), and gentamicin (MIC90e4.0 mg/mL) but resistant to streptomycin (MIC50-64 mg/mL) [40]. Thus, also in this comparison, our functionalized CQDs show some comparable or better behavior than those of some common antibiotics. To identify the factors that govern the trends that we observed for the antibacterial activity of S- and N-doped dots towards each bacterial strain, and to clarify which surface groups facilitate their interaction with the microbial cells, the morphological and surface chemical features of the dots were extensively examined, and are discussed below.

3.2. Characterization of N-CQDs and S-CQDs

One of the proofs indicating the CQDs nature of our samples is their fluorescence. Fig. 3 compares the emission spectra of the S- CQDs and N-CQDs solutions obtained from poly(sodium4-styrene sulfonate) and polyvinylpyrrolidone, respectively) at an excitation wavelength of 350 nm and illustrates the spectra of the two dots. An optical image of the CQDs solutions under UV light irradiation is also included (both solutions exhibit the same color under UV light). A small difference in the pH values of the two samples (3.0 for S-CQDs and 4.5 for N-CQDs) is linked to differences in the sur- face chemistry of the dots, which as aforementioned is extensively discussed below. The quantum yield for S-CQDs and N-CQDs was 9.5% and 6%, respectively, and the details are provided in the Supplementary Information (S.I.). The morphology of the dots was analyzed by high-resolution transmission electron microscopy (HR-TEM). The TEM images are collected in Fig. 4. Both samples consist of well dispersed dots with uniform spherical shapes. The average diameter of the dots is 6.5 nm and 5 nm for N-CQDs and S-QCQDs, respectively. The HR- TEM images indicate that both dots show typical to graphitic car- bon lattice parameters. The surface chemical features of our CQDs were analyzed using Fourier Transform Infrared (FT-IR) spectroscopy. To minimize the spectral contribution of water in aqueous CQDs solutions, the dots were dried and the FT-IR spectra of remaining solids were collected. They are illustrated in Fig. 5. The most important spectral features of S-

CQDs are the four bands between 1000 and 1180 cm^{-1}, characteristic of the symmetric and asymmetric stretching vibration of O S O in eSO_3H and sulfates [41-43], and two bands at 1635 cm^{-1} and 1411 cm^{-1}, indicative of the existence of carboxylic groups [44]. In the case of N-CQDs, a band of a very strong intensity at 1647 cm^{-1} is assigned to a C O stretching vibration in primary and/ or tertiary amides [45,46]. The presence of these species is further verified by a band at 1288 cm^{-1}, assigned to the stretching vibrations of C-N (in amides) [45]. An absorption band at 3421 cm^{-1} is ascribed to a N-H stretching vibration in aromatic amines, primary amines and amides [46]. Two bands at 1370 and 1423 cm^{-1} are linked to the symmetric vibrations of eOH and COO^- groups in carboxylic acids, respectively [46]. For both samples, additional spectral features between 730 and 850 cm^{-1} correspond to tri- and mono-substituted benzenes, and the broader bands at ~675 cm^{-1} for S-CQDs and ~645 cm^{-1} for N-CQDs are characteristic of the stretching vibration of the benzene ring in aromatic compounds.

The FTIR analysis indicates that sulfonic acids and sulfates are the predominant S-containing groups on the surface of S-CQDs, while amide groups (especially tertiary amides), are the predominant N-containing surface functional groups of N-CQDs. On the surface of the latter some amines are also present. Both samples contain carboxylic groups, which are, however, more pronounced for S-CQDs. The surface chemistry of S-CQDs and N-CQDs was further analyzed by XPS. The content of elements in atomic % and the results of the deconvolution of C 1*s*, O 1*s*, S 2*p* and N 1*s* core energy level spectra are summarized in Tables S2 and S3, and in Fig. 6. S- CQDs have twice less carbon compare its content in N-CQDs (30.5 at % vs 76.2 at %f or S-CQDs and N-CQDs, respectively). The contents of heteroatoms (sulfur or nitrogen) are similar for both samples (8.7 at % of S in S-CQDs and 10.6 at % of N in N-CQDs). Those differences in the carbon content might be related to the high content of sodium in S-CQDs (16.7 at %). A very high content of oxygen in S-CQDs (44.1 at % in S-CQDs and 13.2 at % in N-CQDs) suggests the presence of SO_x groups. This and the high content of sodium indicate that sodium sulfonates/sulfates are formed during the synthesis.

The deconvolution of the C 1*s* core energy level spectra for both CQDs shows three contributions at 284.8 eV, 286.0 eV, and 287.6 eV. They are assigned to sp^2 graphitic carbon, C-O (phenolic, alcoholic, etheric), and to carbon in carbonyl and carboxylic groups, respectively. Comparison of two samples indicates that the contribution of carbonyl groups at 287.6 eV is higher for N-CQDs than for S-CQDs (Fig. 6a and d). The high content of carbon in carbonyl groups could be linked to the marked contribution of amide groups in the case of the N-containing sample (Fig. 6f). Indeed, the N 1*s* core energy level spectrum of N-CQDs shows a maximum at 400.2 eV (100%), which is assigned exclusively to amides and/or amino groups. The existent of amides is supported by the high contribution of C O groups and their existence is in agreement with the results obtained from the FTIR analysis. The O 1*s* core level spectrum for both types of CQDs consists of two contributions (Fig. 6b and e). The main contribution of S-CQDs is attributed to oxygen in sulfates and sulfones/sulfonates, while that of N-CQDs e to oxygen in alcohols and carbonyl groups. For S-CQDs, the contribution at 533.2 eV corresponds to C-O in carboxylic/sulfonic groups, while the contribution at 536.8 eV (Fig. 6b), over- lapping with O 1*s* spectra, represents Na KLL. At 533.2 eV some surface water can also be detected. Based on the deconvolution of the S 2*p* core energy level spectra, the contribution at 168.2 eV is assigned to sulfonic acids, and the one at 169.8 eV is assigned to SO^{2-} in sulfates (Fig. 6c). These results are in agreement with the results of the FTIR analysis. The functional groups on the surface are expect to have an effect on the overall charge of our CQDs. The z potential values measured were 6.47 ± 0.67 and 47.18 mV for N-CQDs and S-CQDs, respectively. Even though are negative indicating the predominance of hydroxyl and carboxylate functional groups on the dots surfaces, the sulfonic groups present in the surface of S-CQDs, as indicated by the XPS analysis, leads to the much more negative z potential for this sample, which also brings more stability to this system [47].

3.3. The mechanism of the antibacterial activity

The antibacterial activities of CQDs, and especially of N-CQDs, were analyzed based on the specific surface chemistry (specific configuration of the heteroatoms), surface charge and size of the dots. The collected results indicate that N-CQDs show a greater bactericidal activity compared to S-CQDs (Figs. 1 and 2 and Fig. S1). Moreover, the overall effects of both dots on the Gram- positive *B. subtilis* seem to be greater than those on the Gram- negative *E. coli*. It is plausible to assume that the antibacterial action of N-CQDs involves a chemical effect, which is related to the specific configuration of the heteroatom (certain surface functional groups). As mentioned earlier in this paper, N-containing carbons are known to facilitate the generation of active oxygen species/superoxide ions (O_2^-), which is linked to their electron donating properties [34-36]. Considering that the nature of CQDs does not significantly differ from that of carbon, the active oxygen species are also expected to be formed on N-doped CQDs. They remain on the surface through electrostatic forces [35]. Therefore, it is plausible to assume that if the reactions leading to the formation of O_2^- take place in an aqueous environment, the presence of water facilitates the formation of OH^-. A simultaneous process which involves the contact of the aqueous solution with the latter species and O_2^- leads to the formation of hydroperoxide anions (HO_2^-), as a result of the reductive (electron-donor) function of certain functional groups [35]. Thus, for our N-CQDs, such a performance is expected too, with a strong influence of those oxidants on their antibacterial activity. The active oxygen species, O_2^-, OH^-, HO_2^- are known to cause damage to many aspects/features of cell physiology (e.g. nucleotides, lipids, proteins, metabolites), thus eventually causing cell death [48,49]. Their generation is a result of the electron donating property of the amides/amines present on the surface of N-CQDs. Previous studies have reported that in the

case of *n*-type doped CQDs, the electron transfer processes and formation of oxygen radicals is enhanced, due to the extra free electron incorporation in the carbon dot [50]. Unlike amides and amines which are known to be moderate and strong electron donating groups, respectively, sulfonates and sulfonic acids, which are the main functional groups in the case of S-CQDs, are known to be strong electron withdrawing groups. This property of S-CQDs, likely explains a limited generation of active oxygen species, and thus their lower bactericidal activity compared to that of N-CQDs.

An additional reason for the higher activity of N-CQDs compared to that of S-CQDs, is related to their positive surface charge (protonation) which enhances their electrostatic interactions with negatively charged components of the lipid membrane [51]. As aforementioned, quaternary ammonium compounds are known to be effective antibacterial moieties, disrupting the bacterial cell membranes, and inhibiting the bacterial viability. In our case, the main N-species are amines and amides, and they are expected to be protonated in an aqueous solution, which was shown by the less negative value of the z potential of N-CQDs compared to that of S- CQDs.

The results presented in Fig. 1, Fig. S1 and Fig. 2 show that both dots, and especially S-CQDs, exhibit a higher bactericide ability toward *B. subtilis* than *E. coli*. This selective bactericidal activity towards the Gram-positive bacterium may be related to composition differences in the cell wall of the two bacterial strains (Gram-positive versus Gram-negative), and thus their affinity to interact in different ways with the specific surface functional groups of the dots. Even though both strains have similar cytoplasmic mem- branes consisting of phospholipids and proteins, Gram-positive bacteria has a simpler cell surface that is negatively charged, due to the existence of teichoic acids on the peptidoglycan layer [7]. Those acids, by providing anionic sites, can interact easier through electrostatic interactions with the positively charged N-moieties (originating from the protonation of amines/amides) of N-CQDs, than with the negatively charged S- and O-moieties of S-CQDs. This facilitates the penetration of the former dots into the cell plasma membrane. This is in agreement with previously reported results which indicated that quaternized CQDs shown selective fluores- cence imaging and high bactericidal activity towards Gram-positive bacteria [7].

In the case of S-CQDs, their extensive surface characterization indicated the presence of sulfonic groups, sulfones, sulfates and carboxylic acids. These species dissociate in water, and a strong negative charge inhibits the dots to enter the negatively charged cell walls because of the repelling charges [51,52]. Thus, a lower bactericidal activity against *B. subitlis* in the case of S-CQDs is attributed to their limited electrostatic interactions with the cell membrane. Gram-negative bacteria, such as *E. coli* in our case, have a more complex cell surface structure than Gram-positive bacteria. It consists of a thin peptidoglycan layer between the cytoplasmic membrane and the outer cell membrane, while the latter one consists of lipopolysaccharides (LPS), cross-bridged by divalent cations [7]. Indeed, Gram-negative bacteria are generally more resistant to antibiotics compared to Gram-positive species. Interestingly, the antibacterial effects of both CQDs on this bacterial strain (*E. coli*) are identical regardless the charge or chemistry. Thus, the effect towards *B. subtilis* is likely related to the size of the dots rather than to their electrostatic interactions with the cell membrane.

4. Conclusions

In conclusion, we have demonstrated, through the qualitative disk diffusion approach and MIC quantitative test, that S- and N- containing carbon quantum dots (CQDs), obtained from commodity chemicals by a simple hydrothermal approach, have a capability to act as bactericides against Gram-positive (*B. subtilis*) and Gram-negative (*E. coli*) bacterial strains. Disk diffusion studies revealed a greater effectiveness of N-CQDs compared to S-CQDs. The specific surface chemistry of the dots and their sizes were the main factors governing their complex activity as antimicrobials. The bacterial cell death induced by N-CQDs involved electrostatic interactions between the protonated forms of the nitrogen functional groups and the negatively charged cell membrane with the likely generation of active oxygen species. Amines and amides played the most important role in this process. S-CQDs owing to a mainly negatively charged surface, due to dissociation of sulfonic/carboxylic groups and sulfates, showed a size rather than a chemistry dependent (electrostatic interactions) inhibition of the bacterial growth. A selective antibacterial activity against the Gram-positive rather than the Gram-negative bacterium is likely related to differences in the composition of the cell wall of the two types of bacteria, and thus the affinity of the dots to interact differentially with the specific surface functional groups of the dots. The minimum inhibition concentrations for our CQDs are comparable or smaller than those of some antibiotics or silver nanoparticles.

Acknowledgements

This work was supported by NSF collaborative CBET Grant no. 1133112 (TJB). Fuitful discussions with Prof. Anuradha Janakiraman and the experimental contribution of Ms. Andrea L. Cárdenas- Arevalo are appreciated. The authors would also like to thank Prof. Stephen O'Brien, Julien Lombardi and Frederick Pearsall for ac- commodating our needs to use Thermolyne 6000 furnace. M. Algarra and E. Rodríguez-Castellón thank Project CTQ2015-68951- C3-3-R supported by MINECO and FEDER funds. MA thanks also ARDITI through project M1420-01-0145-FEDER-000005-CQM (Madeira 14-20). TJB is grateful to Fulbright Spain for support.

Appendix A. Supplementary data

Supplementary data related to this article can be found at https://doi.org/10.1016/j.carbon.2018.04.018.

References

[1] S.B. Levy, B. Marshall, Nat. Med. 10 (2004) S122.
[2] S. Chernousova, M. Epple, Angew. Chem. Int. Ed. 52 (2013) 1636.
[3] S. Buffet-Bataillon, P. Tattevin, M. Bonnaure-Mallet, A. Jolivet-Gougeon, Int. J.Antimicrob. Agents 39 (2012) 381.
[4] H. Sun, N. Gao, K. Dong, J. Ren, X. Qu, ACS Nano 8 (2014) 6202.
[5] S.Y. Lim, W. Shen, Z. Gao, Chem. Soc. Rev. 44 (2015) 362.
[6] P. Zuo, X. Lu, Z. Sun, Y. Guo, H. He, Microchim. Acta 183 (2016) 519.
[7] J. Yang, X. Zhang, Y.H. Ma, G. Gao, X. Chen, H.R. Jia, Y.H. Li, Z. Chen, F.G. Wu,ACS Appl. Mater. Interfaces 8 (2016) 32170.
[8] Y. Song, S. Zhu, B. Yang, RSC Adv. 4 (2014) 27184.
[9] H. Tao, K. Yang, Z. Ma, J. Wan, Y. Zhang, Z. Kang, Z. Liu, Small 8 (2012) 281.
[10] T. Feng, X. Ai, G. An, P. Yang, Y. Zhao, ACS Nano 10 (2016) 4410.
[11] X. Liu, J. Pang, F. Xu, X. Zhang, Sci. Rep. 6 (2016) 31100.
[12] S.-S. Liu, C.F. Wang, C.X. Li, J. Wang, L.H. Mao, S. Chen, J. Mater. Chem. C 2(2014) 6477.
[13] Y. Liu, Y. Liu, S.-J. Park, Y. Zhang, T. Kim, S. Chae, M. Park, H.Y. Kim, J. Mater. Chem. A 3 (2015) 17747.
[14] W. Bing, H. Sun, Z. Yan, J. Ren, X. Qu, Small 34 (2016) 4713.
[15] B.S.B. Kasibabu, S.L. D'souza, S. Jha, R.K. Singhal, H. Basu, S.K. Kailasa, Anal.Methods 7 (2015) 2373.
[16] J. Wang, J. Qiu, J. Mater. Sci. 51 (2016) 4728.
[17] W. Wang, L. Cheng, W. Liu, Sci. China Chem. 57 (2014) 522.
[18] L. Hui, J. Huang, G. Chen, Y. Zhu, L. Yang, ACS Appl. Mater. Interfaces 8 (2016)20.
[19] B.Z. Ristic, M.M. Milenkovic, I.R. Dakic, B.M. Todorovic-Markovic, M.S. Milosavljevic, M.D. Budimir, V.G. Paunovic, M.D. Dramicanin, Z.M. Markovic, V.S. Trajkovic, Biomaterials 35 (2014) 4428.
[20] A.K. Roy, S.M. Kim, P. Paoprasert, S.Y. Park, I. In, RSC Adv. 5 (2015) 31677.
[21] B. Le Ouay, F. Stellacci, Nano Today 10 (2015) 339.
[22] M. Guzman, J. Dille, S. Godet, Nanomed. Nanotechnol. Biol. Med. 8 (2012) 37.
[23] Q. Dou, X. Fang, S. Jiang, P.L. Chee, T.C. Lee, X.J. Loh, RSC Adv. 5 (2015) 46817.
[24] C. Zhu, Q. Yang, L. Liu, F. Lv, S. Li, G. Yang, S. Wang, Adv. Mater. 23 (2011) 4805.
[25] N. Kawabata, M. Nishiguchi, Appl. Environ. Microbiol. 54 (1988) 2532.
[26] P. Li, Y.F. Poon, W. Li, H.-Y. Zhu, S.H. Yeap, Y. Cao, X. Qi, C. Zhou, M. Lamrani, R.W. Beuerman, E.T. Kang, Y. Mu, C.M. Li, M.W. Chang, S.S. Jan Leong, M.B. Chan-Park, Nat. Mater. 10 (2011) 149.
[27] D.J. Dwyer, D.M. Camacho, M.A. Kohanski, J.M. Callura, J.J. Collins, Mol. Cell 46(2012) 561.
[28] M.J. Meziani, X. Dong, L. Zhu, L.P. Jones, G.E. Lecroy, F. Yang, S. Wang, P. Wang, Y. Zhao, L. Yang, R.A. Tripp, Y.P. Sun, ACS Appl. Mater. Interfaces 8 (2016)10761.
[29] S. Kang, M. Pinault, L.D. Pfefferle, M. Elimelech, Langmuir 23 (2007) 8670.
[30] W.B. Hu, C. Peng, W.J. Luo, M. Lv, X.M. Li, D. Li, Q. Huang, C.H. Fan, ACS Nano 4(2010) 4317.
[31] H. Ji, H. Sun, X. Qu, Adv. Drug Deliv. Rev. 105 (2016) 176.
[32] O. Akhavan, E. Ghaderi, ACS Nano 4 (2010) 5731.
[33] T. Lammel, P. Boisseaux, M.L. Fernández-Cruz, J.M. Navas, Part. Fibre Toxicol. 10 (2013) 27.
[34] V. V Strelko, V.S. Kuts, P.A. Thrower, Carbon 38 (2000) 1499.
[35] V.V. Strelko, N.T. Kartel, I.N. Dukhno, V.S. Kuts, R.B. Clarkson, B.M. Odintsov,Surf. Sci. 548 (2004) 281.
[36] B. Stöhr, H.P. Boehm, R. Schlögl, Carbon 29 (1991) 707.
[37] N.A. Travlou, J. Secor, T.J. Bandosz, Carbon 114 (2016) 544.
[38] S.A. Salmon, L.J. Watts, Avian Dis. 44 (2000) 85e98.
[39] S. Egger, R.P. Lehmann, M.J. Height, M.J. Loessner, M. Schuppler, Appl. Environ.Micobiol. 75 (2) (2009) 2973e2976.
[40] D.B. Adimpong, K.I. Sorensen, L. Thorsen, B. Stuer-Laurdisen, W.S. Abdelgair, D.S. Nielsen, P.M.F. Derkx, L. Jespersen, Appl. Environ. Microbiol. 78 (2012)7903e7914.
[41] K. Sakurai, E.P. Douglas, W.J. Macknight, Macromolecules 25 (1992) 4506.
[42] P.U. Singare, R.S. Lokhande, R.S. Madyal, Open J. Phys. Chem. 01 (2011) 45.
[43] G. Hélary, F. Noirclère, J. Mayingi, V. Migonney, Acta Biomater. 5 (2009) 124.
[44] M. Zhang, Z. Cheng, T. Zhao, M. Liu, M. Hu, J. Li, J. Agric. Food Chem. 62 (2014)8867.
[45] H. Ding, P. Zhang, T. Wang, J. Kong, H. Xiong, Nanotechnology 25 (2014)205604.
[46] M.J. Kim, X.S. Sun, J. Am. Oil Chem. Soc. 92 (2015) 1689.
[47] R.J. Hunter, Zeta Potential in Colloidal Science. Pricnciples and Applications,Academic Press, UK, 1988.
[48] D.J. Dwyer, P.A. Belenky, J.H. Yang, I.C. MacDonald, J.D. Martell, N. Takahashi, C.T.Y. Chan, M. a Lobritz, D. Braff, E.G. Schwarz, J.D. Ye, M. Pati, M. Vercruysse, P.S. Ralifo, K.R. Allison, A.S. Khalil, A.Y. Ting, G.C. Walker, J.J. Collins, Proc. Natl.Acad. Sci. U.S.A. 111 (2014) E2100.
[49] Z.N. Kashmiri, S.A. Mankar, Int. J. Curr. Microbiol.App. Sci. 3 (2014) 34.
[50] M.K. Barman, B. Jana, S. Bhattacharyya, A. Patra, J. Phys. Chem. C 118 (2014)20034.
[51] K.K.R. Datta, O. Kozák, V. Ranc, M. Havrdová, A.B. Bourlinos, K. Šafářová, K. Holá, K. Tománková, G. Zoppellaro, M. Otyepka, R. Zbořil, Chem. Commun. 50 (2014) 10782.
[52] J.S. Dickson, M. Koohmaraie, R.L. Hruska, Appl. Environ. Microbiol. 55 (1989)832.

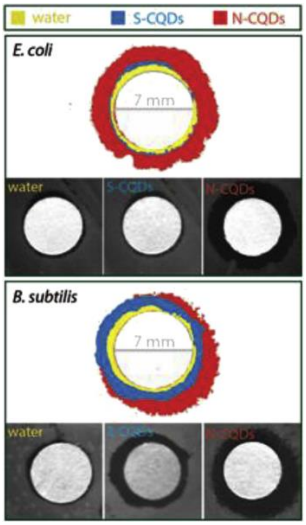

Fig. 1. Diffusion discs assay showing the antibacterial activity of the S-CQDs and N- CQDs against *E. coli* (Gram-negative) and *B. subtilis* (Gram-positive) bacteria. (A colourversion of this figure can be viewed online.)

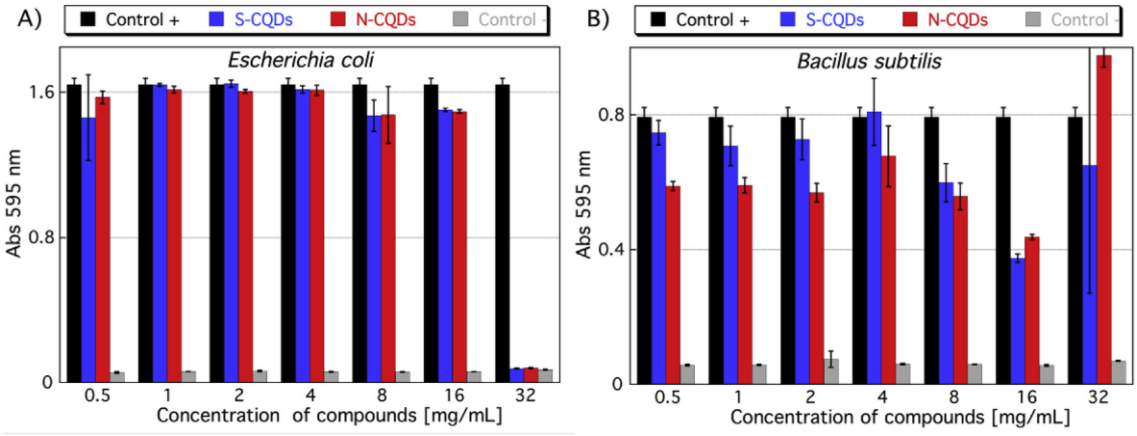

Fig. 2. Minimum inhibitory concentration (MIC) of S-CQDs and N-CQDs on *E. coli* (A) and *B. subtilis* cells (B) after 24 h at 37 °C. Data is presented as the mean values with SD as Error bars. (A colour version of this figure can be viewed online.)

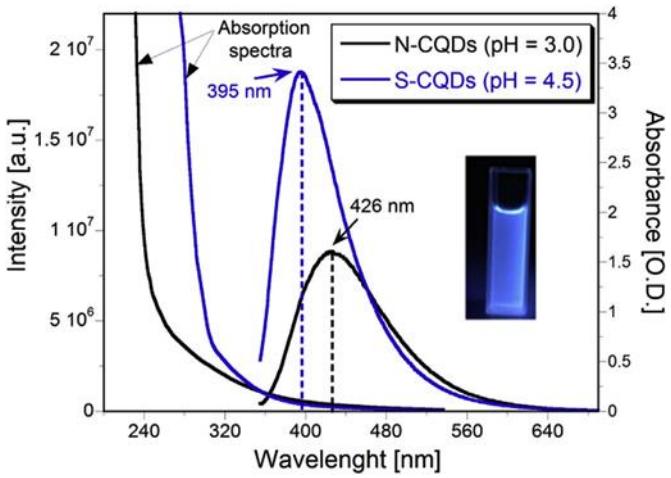

Fig. 3. The emission spectra of S-CQDs and N-CQDs, and the UV-visible absorption spectra of S-CQDs and N-CQDs. The insert is an optical image of the CD solutions at UV light irradiation. (A colour version of this figure can be viewed online.)

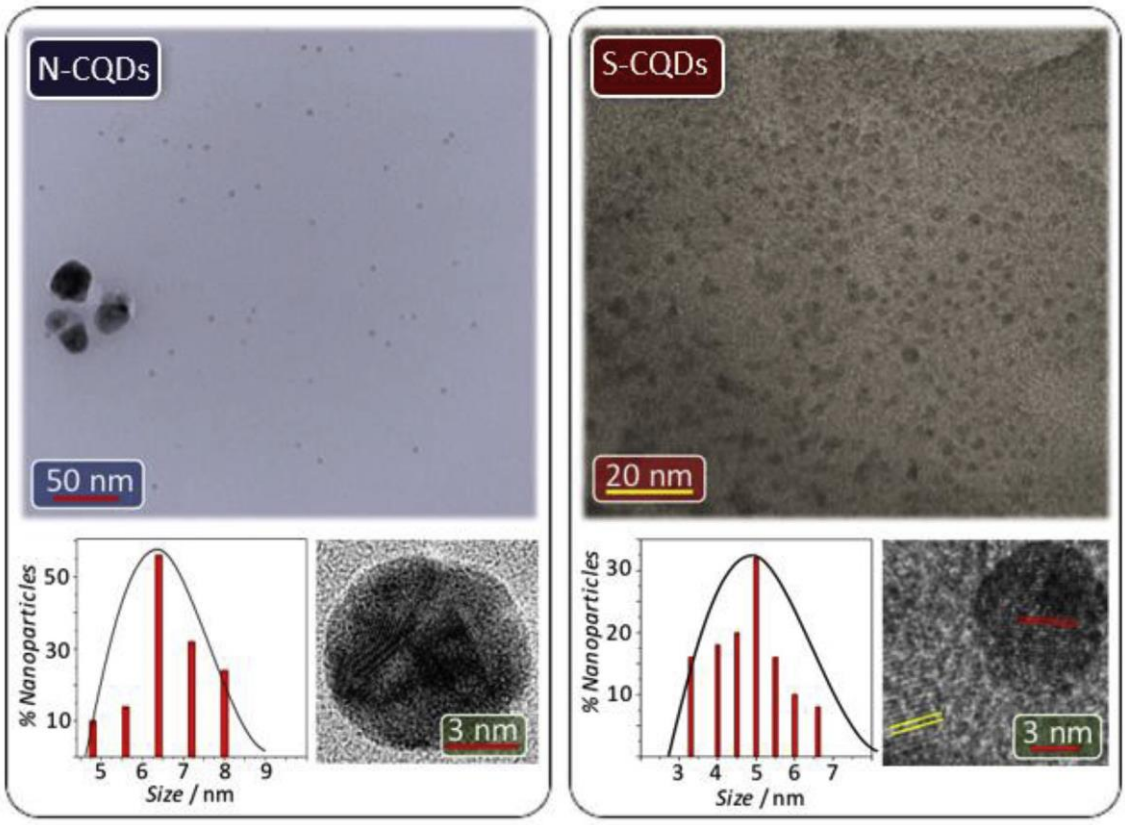

Fig. 4. TEM images of the N-CQDs and S-CQDs. HRTEM images are included as inserts. (A colour version of this figure can be viewed online.)

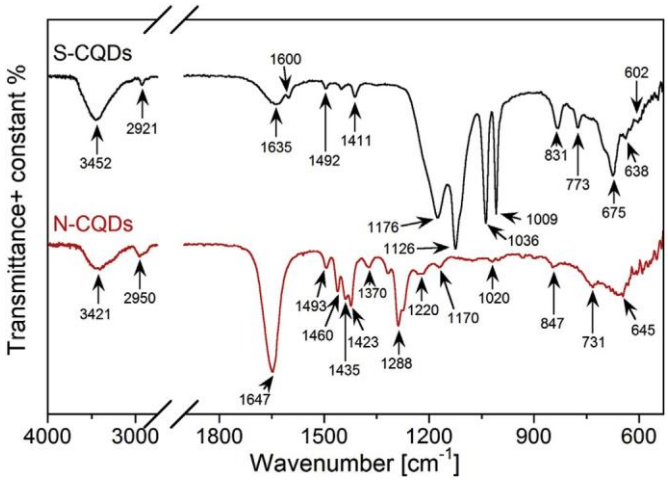

Fig. 5. FT-IR spectra for S-CQDs and N-CQDs after drying. (A colour version of this figure can be viewed online.)

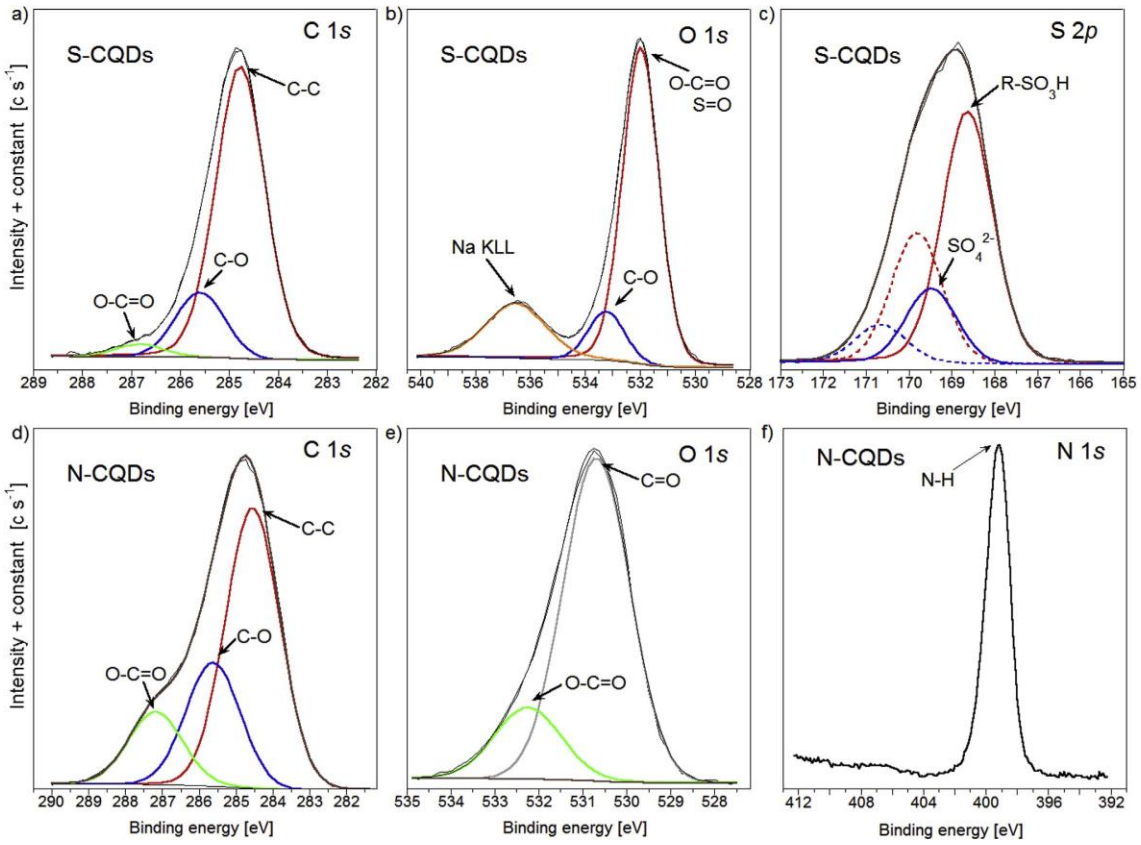

Fig. 6. C 1*s*, O 1*s*, S 2*p*, Na 1*s*, and N 1*s* core level spectra of S-CQDs and N-CQDs. (A colour version of this figure can be viewed online.)